

TABLE IX  
OVERLAP POPULATIONS AND ENERGIES FOR *o*-B<sub>10</sub>H<sub>10</sub>C<sub>2</sub>H<sub>2</sub>  
AND METHYL DERIVATIVES

Bond	<i>o</i> -B <sub>10</sub> H <sub>10</sub> C <sub>2</sub> H <sub>2</sub>	1-Methyl derivative <i>o</i> - B <sub>10</sub> H <sub>10</sub> C <sub>2</sub> H(CH <sub>3</sub> )	1,2-Dimethyl derivative <i>o</i> - B <sub>10</sub> H <sub>10</sub> C <sub>2</sub> (CH <sub>3</sub> ) <sub>2</sub>
C(1)-C(2)	0.645	0.612	0.575
C(1)-B(3)	0.419	0.405	0.435
C(1)-B(4)	0.559	0.534	0.523
C(2)-B(3)	0.419	0.449	0.438
C(2)-B(7)	0.559	0.554	0.520
B(3)-B(4)	0.299	0.338	0.299
B(3)-B(7)	0.299	0.263	0.292
B(3)-B(8)	0.400	0.366	0.328
B(4)-B(5)	0.338	0.375	0.372
B(4)-B(8)	0.482	0.450	0.475
B(4)-B(9)	0.410	0.371	0.362
B(7)-B(8)	0.482	0.509	0.480
B(7)-B(12)	0.410	0.404	0.362
B(8)-B(9)	0.435	0.454	0.444
B(8)-B(12)	0.435	0.427	0.446
B(9)-B(12)	0.383	0.369	0.346
C(1)-methylC(1)		0.912	0.916
C(2)-methylC(2)			0.918
$\Sigma\epsilon_i$	-114.502	-127.743	-140.984
KE <sup>a</sup>	326.607	365.396	404.182
HFMO <sup>b</sup>	-0.382	-0.381	-0.378

<sup>a</sup> Kinetic energy in atomic units. <sup>b</sup> Highest filled molecular orbital in atomic units.

electrophilic attack on *o*-B<sub>10</sub>C<sub>2</sub>H<sub>12</sub> and its C-methyl derivatives.

Overlap populations (Table IX) are reasonable except for the values for C-CH<sub>3</sub> bonds of 0.91 to 0.92, which are to be compared with 0.71 for alkanes.<sup>12</sup> Of course, bond distances do not support partial double-bond character in these C-CH<sub>3</sub> bonds, so we believe that the problem is associated with the *K* value<sup>8</sup> for 2pπ-2pπ overlap. Perhaps this same problem produces the lowered C-C overlap as carborane is methylated. Even so, the B-C overlap populations seem to be unaffected by this symptom, which may be cured when self-consistent field results are available on more appropriate model compounds. Values are also given in Table IX for  $\Sigma\epsilon_i$ , for the kinetic energy, and for the eigenvalue of the highest filled molecular orbital as an estimate of the vertical ionization potential.

Experimental and theoretical studies of these types are being carried out for other carboranes.

**Acknowledgment.**—We wish to thank the Office of Naval Research and the Advanced Research Projects Agency for support of this work. We are also indebted to H. Schroeder for the sample.

(12) M. D. Newton, F. P. Boer, and W. N. Lipscomb, *J. Am. Chem. Soc.* **88**, 2367 (1966).

CONTRIBUTION FROM THE DEPARTMENT OF CHEMICAL ENGINEERING,  
UNIVERSITY OF TEXAS, AUSTIN, TEXAS

## The Crystal Structure of Neodymium Tritelluride<sup>1</sup>

By B. K. NORLING AND H. STEINFINK

Received April 18, 1966

The crystal structure of NdTe<sub>3</sub> has been determined from *h0l* and *0kl* electron density projections and by a least-square refinement of these structure factors. All other reported lanthanide tritellurides are isostructural with it. The crystal is orthorhombic, pseudo-tetragonal, with  $a_0 = b_0 = 4.35$  Å and  $c_0 = 25.80$  Å, space group Bmmb, with four molecules per unit cell. All four crystallographically independent atoms are in position 4(c), 0, 1/4, *z*, of Bmmb. The *z* parameters are 0.8306 (Nd), 0.0705 (Te), 0.4294 (Te), and 0.7047 (Te). The structure is closely related to that of LaTe<sub>3</sub>. The lanthanide atoms in both structures have identical coordination. The NdTe<sub>3</sub> structure may be viewed as a stacking of NdTe<sub>2</sub> unit cells with additional Te layers between cells and with alternate cells shifted by  $a_0/2$ .

### Introduction

The rare earth lanthanides form a series of isostructural compounds of composition LnTe<sub>3</sub>. Pardo, *et al.*,<sup>2</sup> report that Chirazi first prepared CeTe<sub>3</sub> by allowing CeCl<sub>3</sub> to react with H<sub>2</sub> and Te. The product consisted of CeTe<sub>2</sub> and golden, easily cleavable flakes. Carter<sup>3</sup> showed that these crystals had 1:3 stoichiometry, and he prepared also the tritellurides of La and Pr. He noted that their X-ray powder patterns were

identical except for small differences in their cell parameters and from a single-crystal pattern of a disordered LaTe<sub>3</sub> crystal deduced that it was tetragonal,  $a = 4.38$  Å,  $c = 26.10$  Å, with 3 formula weights in the cell. Ramsey, *et al.*,<sup>4</sup> prepared LaTe<sub>3</sub> from the elements and obtained very good, ordered, single-crystal X-ray patterns. The diffraction photographs could be indexed on a tetragonal cell, with four formula weights in the unit cell, but nonspace-group extinctions were observed: *i.e.*, if  $h + k = 2n + 1$ , then reflections with all values of *l* were present; if *h* and *k* were both even, then  $l = 2n$  were present; and if *h* and *k* were both odd,  $l = 2n$

(1) Research sponsored by Air Force Office of Scientific Research, Office of Aerospace Research, U. S. Air Force, Grant No. 808-65, and by National Institute of Health training grant in crystallography, 5T1DE 120-03.

(2) M. Pardo, O. Gorochev, J. Flahaut, and L. Domange, *Compt. Rend.*, **260**, 1666 (1965).

(3) F. N. Carter, "Metallurgy of Semiconductor Materials," Interscience Publishers, Inc., New York, N. Y., p 260.

(4) T. H. Ramsey, H. Steinfink, and E. J. Weiss, *Inorg. Chem.*, **4**, 1154 (1965).

+ 1 were present only. The tetragonal appearance and non-space-group extinctions can be explained on the basis of twinning of an orthorhombic pseudo-tetragonal, B-centered unit cell by reflection across (110). Haase<sup>5</sup> and Lin<sup>6</sup> prepared ErTe<sub>3</sub> and NdTe<sub>3</sub>, respectively, and in both instances the diffraction photographs showed orthorhombic symmetry with  $a = b$  and extinctions which were consistent with space group Bmmb. The most extensive list of lanthanide tritelluride lattice parameters was published by Pardo, *et al.*<sup>2</sup> The compounds were all isostructural although their crystal structure was unknown. We prepared single crystals of untwinned NdTe<sub>3</sub> and investigated its crystal structure.

### Experimental Section

The specimens were prepared by direct reaction of the elements in evacuated Vycor tubes. The methods of preparation have been previously described.<sup>6</sup> The best crystal which was finally chosen for analysis came from a reacted stoichiometric 1:3 mixture. It was a thin, distorted trigonal prism measuring approximately  $40 \times 37 \times 5 \mu$ . The maximum path length of about  $55 \mu$  results in a maximum linear absorption  $\mu_l L = 11.8$  for Cu K $\alpha$  and 1.54 for Mo K $\alpha$  radiation. The crystal was mounted perpendicular to the cleavage plane (001) so that the  $c$  axis was parallel to the spindle axis of the X-ray camera. The  $h0l$  and  $0kl$  reflections were recorded on a precession camera using Mo K $\alpha$  radiation, and the intensities were read by visual comparison with a standard scale. The intensities were corrected for Lorentz and polarization factors, but no absorption corrections were applied. The  $hk0$  and  $hk3$  reflections were recorded using a Weissenberg camera, but these data were used solely to confirm the space group. The systematic extinctions  $hkl$  where  $h + l = 2n + 1$  and  $hk0$  where  $k = 2n + 1$  were consistent with space groups Bmmb, Bm2<sub>b</sub>, or B2mb. The nonstandard orientation was chosen to facilitate comparison of the structure of NdTe<sub>3</sub> to the related structure of LaTe<sub>2</sub>. The unit cell dimensions are  $a = b = 4.35 \text{ \AA}$ ,  $c = 25.80 \text{ \AA}$ ; the measured density of  $7.0 \text{ g/cm}^3$  places 4 formula weights in the unit cell. The structure was solved from an examination of the  $h0l$  and  $0kl$  Patterson projections. With the parameters derived from these projections, structure factors were calculated for the centrosymmetric model, and the essential correctness was confirmed by the agreement between observed and calculated amplitudes and by the appearance of the electron density maps. Refinement was carried out by a least-square procedure using a weighting factor of  $(F_o)^{-2}$  for 120 reflections. All atoms lie in the special position 4(c),  $0, \frac{1}{4}, z$ , at the intersection of two mirror planes in Bmmb. The final value of the discrepancy coefficient,  $R = |\Sigma F_o| - |F_c| / \Sigma |F_o|$ , is 0.125, and Table I shows the atomic coordinates, anisotropic temperature factors, and their standard deviations, for this structure; Table II lists the observed and calculated structure factors.

### Discussion of Structure

The unit cell contains 12 planar layers each consisting of one kind of atom; however, the separation between the neodymium and tellurium layers is  $0.9 \text{ \AA}$  so that they can be considered as one puckered layer. The structure can thus be described as consisting of four puckered layers and four densely packed tellurium layers with the sequence of layers along the  $c$  axis being Te, Nd-Te, Nd-Te, Te, Te, Nd-Te, Nd-Te, Te.

The NdTe<sub>3</sub> structure is closely related to the LaTe<sub>2</sub>

TABLE I  
FINAL COORDINATES,<sup>a</sup> ANISOTROPIC TEMPERATURE  
FACTORS, AND STANDARD DEVIATIONS<sup>b</sup>

Atom	$z$	$B_{11}$	$B_{22}$	$B_{33}$
Te(1)	0.0705 (3)	0.016 (6)	0.020 (5)	0.0005 (1)
Te(2)	0.4294 (3)	0.015 (5)	0.023 (5)	0.0004 (1)
Te(3)	0.7047 (3)	0.013 (5)	0.026 (5)	0.0004 (1)
Nd	0.8306 (3)	0.010 (3)	0.013 (4)	0.0002 (1)

<sup>a</sup>  $x = 0$  and  $y = 0.2500$  for each atom. <sup>b</sup> Numbers in parentheses are standard deviations in the least significant figure.

TABLE II  
OBSERVED AND CALCULATED STRUCTURE FACTORS FOR NdTe<sub>3</sub>

$h$	$k$	$l$	$F_o$	$F_c$	$h$	$k$	$l$	$F_o$	$F_c$
0	0	2	88	-59	1	0	1	65	52
0	0	4	125	-98	1	0	3	97	-76
0	0	6	118	-86	1	0	5	89	-54
0	0	8	476	-855	1	0	7	239	230
0	0	12	182	201	1	0	9	252	-259
0	0	14	240	115	1	0	11	114	117
0	0	16	120	115	1	0	13	130	117
0	0	18	80	64	1	0	15	229	-259
0	0	22	255	-125	1	0	17	204	222
0	0	22	255	-201	1	0	19	54	-54
0	0	24	120	124	1	0	21	89	-85
0	0	28	143	154	1	0	23	113	114
0	0	30	221	226	1	0	25	81	-52
0	0	32	157	-148	2	0	0	418	629
0	1	2	109	83	2	0	2	58	-34
0	1	6	187	-145	2	0	4	101	-73
0	1	8	232	271	2	0	6	79	-59
0	1	10	181	-218	2	0	8	380	-439
0	1	14	195	212	2	0	12	172	169
0	1	18	218	-282	2	0	14	201	208
0	1	18	129	161	2	0	16	105	86
0	1	20	45	30	2	0	18	78	58
0	1	22	121	-122	2	0	20	187	-151
0	1	24	82	85	2	0	22	230	-264
0	2	0	489	-618	2	0	24	120	132
0	2	8	34	30	2	0	28	134	138
0	2	8	88	74	2	0	30	167	204
0	2	6	8	87	2	0	32	138	-130
0	2	6	516	489	2	0	1	41	38
0	2	12	189	-189	2	0	3	77	-56
0	2	14	268	-187	2	0	7	177	160
0	2	16	103	-84	2	0	9	181	-193
0	2	16	94	-59	2	0	11	94	87
0	2	20	146	170	2	0	13	105	87
0	2	20	250	265	2	0	15	188	-208
0	2	24	111	-108	2	0	17	189	172
0	2	28	116	-116	2	0	19	49	-40
0	2	30	183	-198	2	0	21	86	-87
0	2	32	121	127	2	0	23	97	101
0	3	2	86	-60	3	0	25	76	-42
0	3	4	38	32	3	0	0	306	592
0	3	8	309	89	3	0	4	47	-47
0	3	8	164	-161	3	0	8	284	-282
0	3	10	135	149	3	0	12	116	114
0	3	14	143	-151	3	0	14	178	130
0	3	16	173	181	3	0	16	79	62
0	3	18	111	-108	3	0	18	80	45
0	3	22	101	98	3	0	20	115	-121
0	3	24	80	-88	3	0	22	205	-197
0	4	0	318	351	4	0	24	95	87
0	4	8	289	-283	4	0	28	36	-37
0	4	12	113	118	4	0	7	108	102
0	4	14	185	111	4	0	9	123	-122
0	4	16	54	58	4	0	11	60	59
0	4	20	117	-117	4	0	15	40	56
0	4	22	178	-184	4	0	17	147	-148
0	4	24	79	78	4	0	17	110	110
0	5	0	102	104	5	0	21	80	-48
0	5	10	101	-88	5	0	0	0	0
0	5	14	89	89	5	0	0	0	0
0	5	18	111	-115	5	0	0	0	0
0	5	18	86	59	5	0	0	0	0

structure discussed by Wang, *et al.*,<sup>7</sup> and the two structures are compared in Figure 1. The NdTe<sub>3</sub> structure may be visualized as a stacking of slightly distorted NdTe<sub>2</sub> unit cells having an additional tellurium layer between adjacent cells, with alternate cells shifted by  $a_0/2$ . The Nd coordination in NdTe<sub>3</sub> is identical, except for a small difference in bond length, with that in NdTe<sub>2</sub>. The interatomic distances in NdTe<sub>3</sub> and LaTe<sub>2</sub> are compared in Table III.

The phase NdTe<sub>2</sub> displays a solid-solution region, with the other terminal composition near NdTe<sub>1.7</sub>, and the tellurium deficiency results from the removal of Te from the pure tellurium layers, *i.e.*, those equivalent to the Te(1) and Te(2) layers in the NdTe<sub>3</sub> structure.<sup>7</sup> Since the conductivity of NdTe<sub>2</sub> is the highest of the solid-solution series, it was concluded that the pure tellurium layers account for most of the metallic behavior of the compounds. The apparent radius of tellurium in the pure tellurium layers of NdTe<sub>3</sub> is  $1.538 \text{ \AA}$ , which is near the accepted metallic radius of  $1.60 \text{ \AA}$  for 12-fold coordinated tellurium. From Figure 1 it is clear that NdTe<sub>3</sub> contains twice as many tellurium

(5) D. J. Haase, H. Steinfink, and E. J. Weiss, *Inorg. Chem.*, **4**, 541 (1965).

(6) W. Lin, H. Steinfink, and E. J. Weiss, *ibid.*, **4**, 877 (1965).

(7) R. Wang, H. Steinfink, and W. F. Bradley, *ibid.*, **5**, 142 (1966).

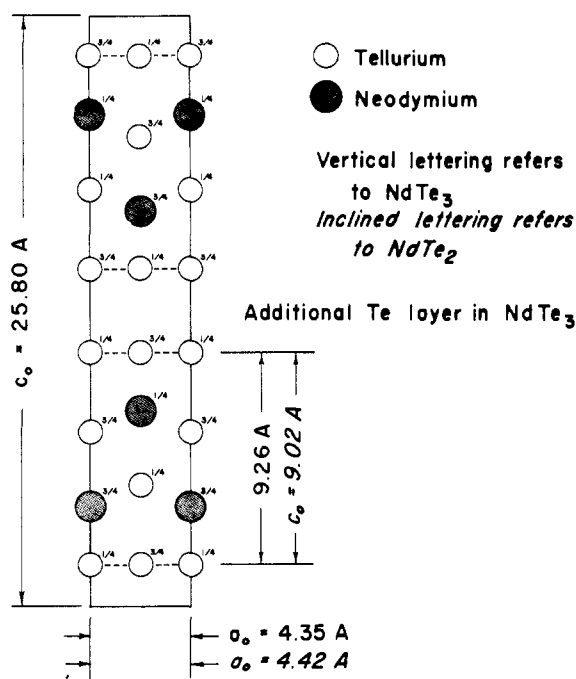


Figure 1.—A comparison of the structures of  $\text{NdTe}_3$  and  $\text{NdTe}_2$  in the  $h0l$  projection.

TABLE III  
A COMPARISON OF INTERATOMIC DISTANCES  
IN  $\text{NdTe}_3$  AND  $\text{LaTe}_2$

Interatomic distances, A	NdTe <sub>3</sub>		LaTe <sub>2</sub> <sup>a</sup>
Te(1)–Te(1)	4.240	± 0.010	ne <sup>a</sup>
Te(2)–Te(2)	4.350	± 0.010	ne
Te(3)–Te(3)	3.862	± 0.010	4.009
Te(1)–Te(2)	3.076	± 0.010	3.187
	4.240	± 0.010	ne
Te(1)–Te(3)	4.089	± 0.010	4.036
Te(2)–Te(3)	4.089	± 0.010	4.033
Nd–Nd	4.350	± 0.009	4.507
Nd–Te(1)	3.353	± 0.010	3.381
Nd–Te(2)	3.353	± 0.010	3.381
Nd–Te(3)	3.208	± 0.009	3.293
	3.246	± 0.009	3.260

<sup>a</sup> ne: no equivalent interatomic distance reported for  $\text{LaTe}_2$ .

atoms in the pure tellurium layers as does  $\text{NdTe}_2$ . It might be concluded, as a first approximation, that lanthanide tritellurides should exhibit twice the metallic character of lanthanide ditellurides. Although this assumption depends on a structural analogy which ignores detailed differences in bonding within the pure tellurium layers, it is supported by experiments. Ramsey<sup>8</sup> measured the resistivities of similarly processed samples of  $\text{LaTe}_2$  and  $\text{LaTe}_3$ . Over the range  $-50$  to  $+270^\circ$ , the resistivity of  $\text{LaTe}_3$  ranged from about 0.3 to 0.7 of that of  $\text{LaTe}_2$ .

There are essentially only two types of tellurium and one type of neodymium present. Te(1) and Te(2) have identical coordination polyhedra. Each Te(1 or 2), Figure 2, is surrounded by six nearest neighbors, at 3.076 Å (4 Te) and at 3.353 Å (2 Nd), forming an ir-

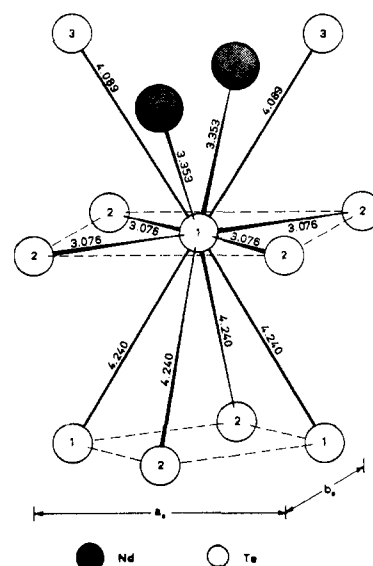


Figure 2.—Te(1) or Te(2) coordination polyhedron; distances are shown in Å.

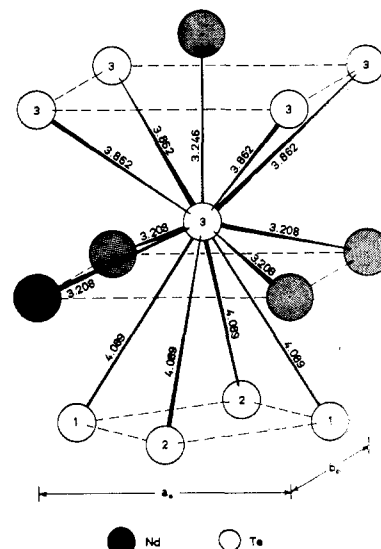


Figure 3.—Te(3) coordination polyhedron; interatomic distances are shown in Å.

regular prism. The other tellurium atoms in Figure 2 cannot be considered as bonded to the central Te atom. The remaining third of the tellurium atoms, Te(3), Figure 3, are each surrounded by five nearest neighbors at 3.208 Å (4 Nd) and 3.246 Å (1 Nd), forming a nearly regular pyramid; the other atoms shown are considered as nonbonded because of the large interatomic distances. Each neodymium, Figure 4, is surrounded by nine near neighbors at 3.208 Å (4 Te), 3.256 Å (1 Te), and 3.353 Å (4 Te). The nearest Nd–Nd approach is 4.35 Å, and these distances are parallel to the  $a_0$  and  $b_0$  axes.

The bond numbers may be calculated from Pauling's equation for intermetallic compounds

$$D(n) = D(1) - 0.600 \log n$$

where  $D(n)$  is the observed bond distance for bond number  $n$ ,  $n$  less than 1.0 for intermetallic compounds,

(8) T. H. Ramsey, H. Steinfink, and E. J. Weiss, *J. Appl. Phys.*, **36**, 548 (1965).

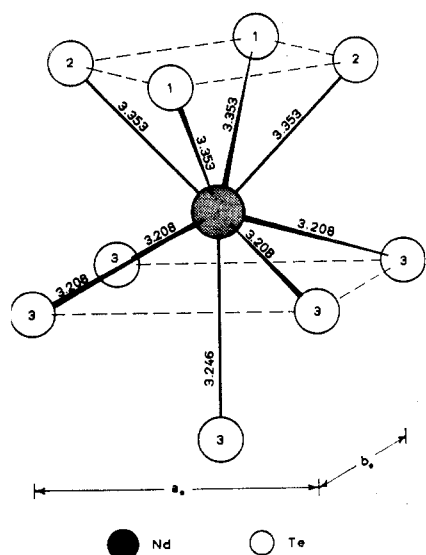


Figure 4.—Neodymium coordination polyhedron; interatomic distances are in Å.

and  $D(1)$  is the empirically determined single-bond distance, the sum of the single-bond radii,  $R(1)$ , of the

two atoms involved. Pauling's values of  $R(1)$  for neodymium and tellurium are 1.637 and 1.37 Å, respectively.<sup>9</sup> The bond numbers and corresponding valences are summarized in Table IV. It should be noted that the calculated valence for the "metallic-covalent" tellurium atoms is considerably less than the formal valence for  $\text{Te}^{2-}$ .

TABLE IV  
BOND DISTANCES, BOND NUMBERS, AND VALENCES

Central atom	Coordinating atom	$D(n)$	$n$	$\Sigma n$ (valence)
Nd	4 Te(3)	3.208	0.462	
	1 Te(3)	3.246	0.399	
Te(1 and 2)	4 Te(1 and 2)	3.353	0.265	3.307
	4 Te(1 or 2)	3.076	0.275	
	2 Nd	3.353	0.265	
	2 Te(3)	4.089	0.006	
Te(3)	4 Te(1 and 2)	4.240	0.003	1.654
	4 Nd	3.208	0.462	
	1 Nd	3.246	0.399	
	4 Te(3)	3.862	0.014	
	4 Te(1 and 2)	4.089	0.006	2.323

(9) L. Pauling, "The Nature of the Chemical Bond," 3rd ed, Cornell University Press, Ithaca, N. Y., 1960, p 403.

CONTRIBUTION FROM BELL TELEPHONE LABORATORIES, INCORPORATED,  
MURRAY HILL, NEW JERSEY

## Crystallographic Evidence for Nonequivalent Ligand Fields in Tantalum Subchloride

By R. D. BURBANK

Received April 18, 1966

Robin and Kuebler have interpreted the electronic spectra of the polynuclear subhalides of tantalum of general formula  $\text{Ta}_6\text{X}_{14} \cdot 7\text{H}_2\text{O}$  in terms of a distorted polynucleus in which two Ta at the apices of an elongated tetragonal bipyramid approach a valence of +3 while four Ta in the equator of the bipyramid approach a valence of +2. An X-ray structure analysis of  $\text{Ta}_6\text{Cl}_{14} \cdot 7\text{H}_2\text{O}$  crystals is consistent with this interpretation. The crystals are trigonal, most probable space group  $\text{P}\bar{3}1\text{m}$ , with  $a = 9.36$  Å,  $c = 8.80$  Å, and one unit of composition per unit cell. The structure, which is both disordered and subject to faulting, contains an elongated bipyramidal polynucleus. One type of ligand field is provided for two Ta along the axis of elongation, and a second type of ligand field is provided for the remaining four Ta. The polynucleus combines with twelve Cl to form a  $\text{Ta}_6\text{Cl}_{12}^{2+}$  complex ion. The complex ion combines with two Cl ions and four  $\text{H}_2\text{O}$  to form a  $\text{Ta}_6\text{Cl}_{14} \cdot 4\text{H}_2\text{O}$  unit. The  $\text{Ta}_6\text{Cl}_{14} \cdot 4\text{H}_2\text{O}$  units occur in layers which alternate with layers of three  $\text{H}_2\text{O}$  to yield the over-all composition of  $\text{Ta}_6\text{Cl}_{14} \cdot 7\text{H}_2\text{O}$ . The observed structural disorder appears to be built into the crystal during the course of crystal growth in order to permit a maximum of hydrogen bonding throughout the crystal.

### Introduction

In a recent study of color and nonintegral valence Robin and Kuebler<sup>1</sup> have concluded that there is a fundamental difference between the niobium and tantalum subhalides. The compounds have the general formula  $\text{M}_6\text{X}_{14} \cdot 7\text{H}_2\text{O}$  where  $\text{M} = \text{Nb}$  or  $\text{Ta}$  and  $\text{X} = \text{Cl}$ ,  $\text{Br}$ , or  $\text{I}$ . The central building block in these compounds is the polynuclear complex ion  $\text{M}_6\text{X}_{12}^{2+}$ . Vaughan, Sturdivant, and Pauling<sup>2</sup> determined the structures of the ions  $\text{Nb}_6\text{Cl}_{12}^{2+}$ ,  $\text{Ta}_6\text{Br}_{12}^{2+}$ , and  $\text{Ta}_6\text{Cl}_{12}^{2+}$  in

ethanol solutions using X-ray diffraction. Within the limitations imposed by the experimental technique, the scattering was satisfactorily explained by a model of cubic symmetry. The metal atoms are situated at the corners of an octahedron whose edges are  $\sim 2.9$  Å long. The halide atoms are on the radial perpendicular bisectors of the octahedral edges with a metal to halogen distance of  $\sim 2.4$  Å.

In the octahedral model of the  $\text{M}_6\text{X}_{12}^{2+}$  ion, the metal atoms are all in equivalent ligand fields within the complex and the formal valence at each metal atom is  $+2\frac{1}{3}$ . However, if the symmetry is lower than octa-

(1) M. B. Robin and N. A. Kuebler, *Inorg. Chem.*, **4**, 978 (1965).

(2) P. A. Vaughan, J. H. Sturdivant, and L. Pauling, *J. Am. Chem. Soc.*, **72**, 5477 (1950).